Hystrix, (n.s.) 11 (1) (2000): 9-25

ON THE USE OF SHAPE SPACES TO COMPARE MORPHOMETRIC METHODS

F. JAMES ROHLF

Department of Ecology and Evolution
State University of New York
Stony Brook, NY 11794-5245
roh&2life.bio.sunysb.edu

ABSTRACT - Several methods have been proposed to use differences in configurations of landmark points to measure the amount of shape difference between two structures. Shape difference coefficients ignore differences in the configurations that could be due to the effects of translation, rotation, and scale. One way to understand the differences between these methods is to compare the multidimensional shape spaces corresponding to each coefficient. This paper compares Kendall's shape space, Kendall tangent space, the shape spaces implied by EDMA-I and EDMA-II test statistics, the shape space of log size-scaled inter-landmark distances, and the shape space implied by differences in angles of lines connecting pairs of landmarks. The case of three points in the plane (i.e., landmarks at the vertices of a triangle) is given special emphasis because the various shape spaces can be illustrated in just 2 or 3 dimensions. The results of simulations are shown both for random samples of all possible triangles as well as for normally distributed independent variation at each landmark. Generalizations to studies of more than three landmarks are suggested. It is shown that methods other than those based on Procrustes distances strongly constrain the possible results obtained by ordination analyses, can give misleading results when used in studies of growth and evolutionary trajectories.

Keywords: Kendall shape space; tangent space: EDMA; inter-landmark distances; multivariate analysis: morphometrics: Procrustes distance; thin-plate spline.

INTRODUCTION

The field of geometric morphometrics represents an important new paradigm for the statistical study of variation and covariation of the shapes *of* biological structures. The notion of shape of used here is that of the relative positions of points corresponding to morphological landmarks. The positions of the points can be captured conveniently by their coordinates (2 for images or 3 for the actual organism). The coordinates must, of course, be recorded in a way such that they are unaffected by variation in a specimen's location, orientation, and scale. The analysis of the shapes of outlines will not be considered here. Rohlf and Marcus (1993) give a general overview of the field of geometric morphometrics. Bookstein (1991) gives a comprehensive account while Small (1996) covers mathematical details. Dryden and Mardia (1998) cover many aspects of shape statistics. (Rohlf, 1999a) discusses some of the interrelationships between methods based on Kendall's shape space. Marcus et al. (1996) includes both introductory material and examples of applications to many fields of biology and medicine. The fundamental advances of geometric morphometrics over traditional approaches (multivariate morphometrics, e. g., Reyment et al., 1984) are in the development of powerful statistical methods based on models for shape variation rather than the use of standard multivariate methods on ad hoc collections of distances, angles, and ratios.

Two rather different approaches for the statistical analysis of shape have been used.

1. Analyses that can be interpreted in terms of the differences in the coordinates of the landmarks after the configurations of points have been optimally superimposed (usually using least-squares).

These methods use the Procrustes distance (the square root of the sum of squared differences) as a metric for comparing shapes. There has been a considerable work in this area using the perturbation model described by Goodall (1991). The exact distribution has even been worked out for certain cases (see Dryden and Mardia, 1998, for a discussion). Kendall (1981; 1984; 1985) has done important initial work. Bookstein (1991), Small (1996) and Dryden and Mardia (1998) are recent texts. Note that the thin-plate spline methods (Bookstein, 1991) are based on this approach.

2. Analyses based on interlandmark distances.

An example is Euclidean Distance Matrix Analysis, EDMA, proposed by Lele and Richtsmeier (1991) and further elaborated in Lele (1993), Lele and Cole (1996), and Richtsmeier and Lele (1993). This approach uses matrices of all pairs of inter-landmark distances. Statistical tests based on bootstrap procedures are used because analytical results are not available and simple normal approximations are not appropriate. Rao and Suryawanshi (1996) and Richtsmeier et al. (1998) proposed using logs of size-scaled inter-landmark distances as shape variables. Recently, Rao and Suryawanshi (1998) suggested the use of angles from triangulation of triplets of landmarks. These latter approaches do not seem to be based on any explicit model for shape variation and assume that their shape variables are at least approximately multivariate normal.

One of the purposes of this study is to contrast some of the statistical consequences of using these approaches. This will be done by comparing the shape spaces implied by the various coefficients used to test for differences in shape. Rao and Suryawanshi (1996) state that there is no unique way of choosing among alternative shape functions and that inference based on a particular choice of functions will be consistent with that based on another choice provided the probability distribution can be accurately specified. However, it would be difficult to relate the exact Mardia-Dryden distributions (see Dryden and Mardia, 1998) to the EDMA statistics. The different methods do not have the same statistical power against various alternative hypotheses (Rohlf 2000). In fact the different approaches do not even obtain the same estimates of the mean shape. Thus these approaches are not equivalent in practice and naive applications of the various methods may lead to very different conclusions.

Most of the figures presented below were generated using the tpsTri software (Rohlf 1999b) that runs under Windows 95/98/NT. It can be downloaded from the Stony Brook morphometrics www site *(http://life.bio.sunysb.edu/morph)* and used to further investigate the morphometric methods described below.

SHAPE DIFFERENCES AND SHAPE SPACES

Several coefficients have been proposed that measure the difference between the shapes of a pair of objects. Table 1 lists the coefficients that will be considered here. While any of these coefficients can be used to develop valid tests for the null hypothesis that two populations have the same mean shape, tests based on different coefficients will differ in their sensitivities to alternative hypotheses (Rohlf 2000). One way to understand these differences in power is to examine the shape spaces implied by the use of these coefficients. One expects statistical power to be lower for distinguishing shapes that are similar according to a particular coefficient. The case of $p=3$ landmarks in $k=2$ dimensions will be emphasized because the shape spaces

Table 1. Shape spaces for triangles.

Name	Distance coefficient	Reflections	Representing surface
Kendall	Procrustes distance, d or ρ	Included	Surface of sphere, radius = 1/2
Space of preshapes aligned to a reference	Procrustes distance, d or ρ	Included	Surface of hemisphere, radius = 1
Kendall tangent space	Euclidean distance using orthogonal projection of hemisphere	Included	Flat disk, radius = 1
EDMA-I	T = ratio of the largest to the smallest of the ratios in the form difference matrix	Ignored	Approximated using principal coordinates of $\ln(T)$
EDMA-II	Z = largest absolute value of differences in size-scaled interlandmark distances	Ignored	Approximated using principal coordinates of $\mathbf{Z}$
Rao & Suryawanshi 1996	Euclidean distance using two linear combinations of log size-scaled interlandmark distances	Ignored	Subset of $\mathbf{R}^2$
Rao & Suryawanshi 1998	Euclidean distance using two interior angles	Ignored	Subset of $\mathbf{R}^2$

can be visualized in 2 or 3 dimensions and thus one can appreciate some of their properties intuitively. For more than three landmarks the shape spaces become high dimensional and for some coefficients their metric geometry becomes much more complicated, Another application of these shape difference coefficients is in multivariate ordination analyses. Matrices of these coefficients can be used directly in Principal coordinates analysis and various types of multidimensional scaling analysis (see, for example, Jackson, 1991). Because the user will attempt to interpret any patterns found in such ordinations, the space should not constrain the distribution of points so as to introduce apparent structure in the data when none is actually present. This will be shown to be a problem for the methods based on interlandmark distances.

Procrustes distance

This type of shape distance between a pair of configurations of landmark points is usually computed by first centering the two configurations of landmarks on the origin and scaling each configuration to unit centroid size (the square root of the sum of their squared coordinates, Bookstein, 1991). One of the configurations is then rotated to align it with the other so that d, the square root of the sum of squared differences between corresponding coordinates, is as small as possible. This quantity, d, is often called a Procrustes distance but there is a related quantity, ρ, to which this term is also applied (see below). Gower (1975) gives a general matrix algorithm to align one set of points to another. Bookstein (1991) gives an efficient method for 2-dimensional data using com-

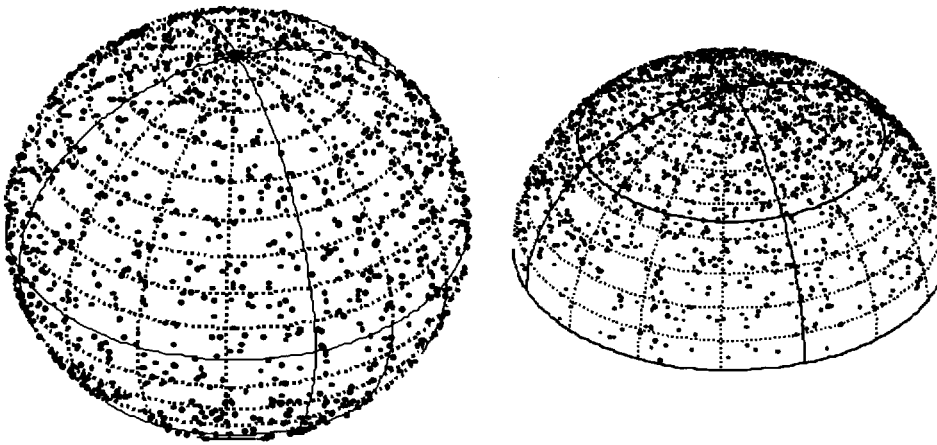

A B

Figure 1. Shape spaces for triangles in the plane. *A.* Kendall's shape space for triangles. The points show the positions of 2000 random triangles on the surface of a sphere. *B.* Space of shapes aligned to a reference shape. Points on the surface of the hemisphere correspond to the same sample of 2000 triangles.

plex correlation. Procrustes distances are also used to compare multivariate ordinations where it makes sense to reflect axes if that would improve the fit (because the orientations of multivariate axes are usually arbitrary). In morphometrics reflections should not be performed automatically because differences that appear as reflections may actually be part of the overall shape difference (see Goodall, 1991, and Rohlf, 1996). Of course if one has sampled, for example, a mixture of left and right insect wings then will need to reflect some specimens in order for them to be aligned in a consistent way. In multivariate applications it may also be useful to allow the size of one configuration to shrink to cos p because that will improve the fit by reducing d to sin ρ. This is called a full Procrustes fit by Dryden and Mardia (1998). Cole (1996) reviews some early uses of this coefficient.

Kendall (1981; 1984) showed that the shape space corresponding to the Procrustes metric is a kp-k-1-$k(k$-1)/2 - dimensional manifold ($2p$-4 dimensions for 2D and $3p$-7 dimensions for 3D). A manifold is a generalization to higher dimensions of a curved surface in 3 dimensions. Small (1996) gives an introduction to the topic and discusses applications to morphometrics. For p=3 and k=2 (triangles in the plane) the manifold corresponds to the surface of an ordinary sphere with radius 1/2 (this is a 2-dimensional curved space). Every possible shape maps to a unique position in Kendall shape space. Because this space for triangles corresponds to the surface of a sphere it seems natural to consider measuring the distance between shapes as geodesic (great circle) distances, p, rather than as chord distances, d, from a partial Procmstes fit. These two quantities are related as $p = 2\sin^{-1}(d/2)$ because ρ is also the angle between vectors connecting the points with the center of the GLS hemisphere (see below). The maximum value for p is $\pi/2$ (the distance between an object and the shape maximally different from it). Figure 1A depicts this

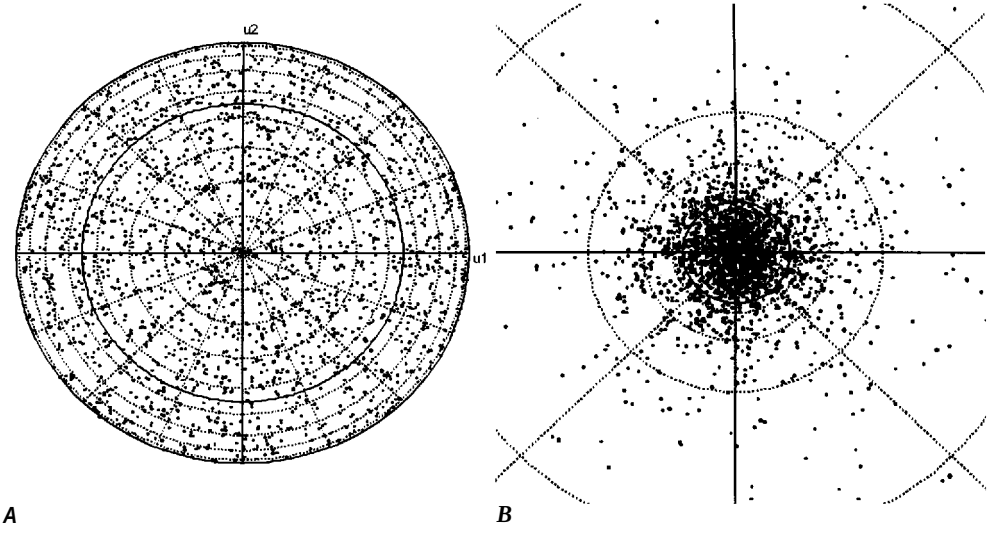

Figure 2. Tangent spaces. ***A.*** An orthogonal projection of the GLS space of preshapes aligned to the reference shape (see Figure 1B). The central point corresponds to the reference or point of tangency, the pole in Figure 1B. *B.* Stereographic projection of Kendall's shape space in Figure 1A. The center corresponds to the reference or point of tangency, the North pole in Figure 1A. A point at the South pole becomes a point at infinity.

space with points corresponding to a random sample of 2000 triangles superimposed. The distribution of points on this surface is uniform (Kendall, 1985). Because this shape space is curved it has a non-Euclidean geometry and special statistical methods have to be used. For example, Goodall (1991) developed a statistical test based on ratios of squared Procrustes chord distances.

An important property of manifolds is that for small variation (i.e., locally) they can be approximated by an Euclidean tangent plane. Thus one can construct a linear approximation to shape space by projecting points from shape space onto an Euclidean tangent space that has the same number of dimensions as shape space. If shape variation is sufficiently small (shapes distributed in a small region around the point of tangency), then no information is lost. The point corresponding to the average shape is usually used as the point of tangency because that provides the best approximation. Standard linear multivariate methods can then be used on the data points in the tangent space. Two projection methods are commonly used: stereographic projection of Kendall shape space (Bookstein shape coordinates are a special case, Small, 1996) and an orthogonal projection of the GLS hemisphere. The GLS hemisphere (see Figure 1B) is the space one obtains when all triangles are least-squares aligned to a reference shape. It is a hemisphere with radius 1 (or a hyper-hemisphere if $p>3$, see Rohlf, 1999a). Figure 2A illustrates the orthogonal projection of the GLS hemisphere shown in Figure 1B onto a plane tangent its Pole (equivalent to a top view of the hemisphere). Kent (1994) calls this space Kendall tangent space (but Dryden and Mardia, 1992, call it Kent tangent space). Note that the density of points in the Kendall tangent space appears uniform. Figure 2B shows the results of a stereographic projection. The points are concentrated near the origin of this space. Not all points are shown because those at

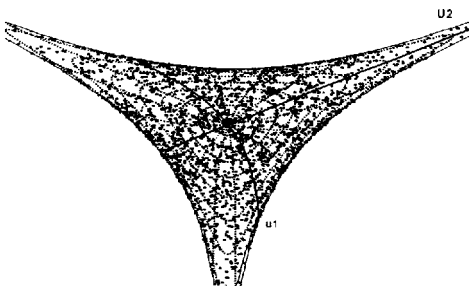

Figure 3. Shape space **for** triangles using shape variables based on logs of interlandmark distances as defined by Rao and Suryawanshi (1996). The center corresponds to an equilateral triangle. The points correspond to a random sample of 2000 triangles.

the point opposite the point of tangency map to infinity. Polar coordinates were used in Figure 2 to emphasize the relationships to the hemisphere and sphere in Figure 1. In practice the tangent.space is overlaid with a Cartesian coordinate system (partial warps are one example).

Distance in log inter-landmark distance space

Rao and Suryawanshi (1996) proposed comparing shapes using distances based on the logs of the distances between all pairs of landmarks. Specifically, they used

$$\mathbf{d}^{(s)} = \mathbf{H}\mathbf{d} \qquad (1)$$

as a set of m-1 shape variables, where $\mathbf{d}$ is the vector of logs of the m distances between pairs of landmarks, $\mathbf{H}$ is an $(m - 1) \times m$ matrix of rank m-1 such that $\mathbf{H1} = \mathbf{0}$ (a Helmert matrix with the first row deleted), and $m = (p - 1)p/2$ (the number of distances between pairs of landmarks). Equation 1 projects the vector of distances onto a space orthogonal to their mean (thus size-scaling by removing the log of the geometric mean distance). The matrix $\mathbf{H}$ is not unique. However, the rows are orthogonal so different choices simply correspond to rotations of the space (which have no effect on distances between shapes). Richtsmeier et al. (1998) proposed an equivalent shape difference — the Euclidean distance between shapes using logs of scaled distances as variables. Rao and Suryawanshi (1996) proposed the use of traditional multivariate analyses on the resultant shape variables. For example, they used generalized distance to quantify the amount of difference in shape between two samples. It is easy to depict the implied shape space for triangles in the plane because Equation 1 generates just two shape variables in this case (m-1=2). Figure 3 was prepared by projecting points corresponding to triangles along the latitude and longitude lines in the upper half of the sphere in Figure 1A. Points corresponding to a random sample of 2000 triangles are superimposed. As in the case of the EDMA-I and EDMA-II methods described in the next section, shapes and their reflections map to the same point (i.e., differences due to reflection are ignored). A point at the center of this space corresponds to an equilateral triangle and the three arms correspond to the three kinds of isosceles triangles (the arms extend to infinity as the base of an isosceles triangle goes to zero). For p>3 the space will require more dimensions and will be more complicated and difficult to visualize. There will be m arms extending out to infinity with "webs" connecting pairs, triples, *etc.* of arms corresponding to one, two, etc. inter-landmark distances going to zero. Another complication is that the central point in the space corresponds to a shape with equal inter-landmark distances. However, for p>3 (2D data) or p>4 (3D data) such shapes are not physically realizable. Such shapes cannot be a part of a shape space and thus there is a gap in the center of this space that should be taken into account by any statistical methods. It is interesting to attempt to visualize the case of 4 landmarks in the plane. The space will be 5-dimensional because $m = 4 \times 3/2 = 6$. There will be 6 arms extending to infinity. At infinity the cross-section of each arm will re-

semble Figure 3 (because, with one distance equal to zero, the remaining possible variation correspond to that of a triangle). The central point in this space corresponds to a shape with all 4 inter-landmark distances equal to one another (which is not possible for a configuration of points in 2D) so there must be a gap at the center of this space.

Euclidean distance matrix analyses, EDMA-I and EDMA-II

This approaches uses as variables all $m = p(p-1)/2$ distances between pairs of landmarks. Euclidean distances are influenced by size but not by the effects of differences in translation and orientation of an object. However, they are also not sensitive to shape differences that appear to be due to reflections (see Rohlf, 1996). These variables allow an object to be represented as a point in an m-dimensional form space (it is a form space rather than a shape space because variation in size has not been removed, Goodall, 1991). Richtsmeier and Lele (1993) attempt to illustrate this space but, unfortunately, they show the region corresponding to form space upside down and to the wrong relative scale. Note that, except for p=3 and k=2, the space is of unnecessarily high dimensionality. Only $kp - k - (k-1)k/2$ dimensions are required for form space. For example, for p=4 and k=2, m=6 although just 5 dimensions are needed. For more landmarks the difference is much greater. For example, for p=25 and k=2, m=300 even though only 47 dimensions are needed.

Lele and Richtsmeier (1991) define a *form difference matrix* to compare two objects. It is made up of the ratios of the corresponding inter-landmark distances for the two objects. They use the statistic T (the ratio of the largest to the smallest of the ratios in the form difference matrix) to test for shape differences between the two objects. Lele and Cole (1995; 1996) refer to this approach as EDMA-I. When comparing two samples of objects they use average distances within each sample. Lele (1993) provides an improved method for estimating the average distances. Both methods use the actual distances rather than size-scaled distances. That means, of course, that an average shape will be determined mostly by the shapes of the largest objects.

It is useful to investigate the shape space implied by the use of T in order to understand some of its statistical properties. This seems difficult to do analytically so the following numerical procedure was used. A systematic sample of 62 triangles that covered the space of all possible triangles (excluding reflections) was generated and a 62x62 matrix of $\ln(T)$ values generated. **A** Principal Coordinates Analysis' (Gower, 1966) was then performed on this matrix to obtain the best 3-dimensional Euclidean view of the implied shape space. The add-a-point technique (Gower, 1968) was then used to project into this space points corresponding to triangles along the latitude and longitude lines in the upper half of the sphere in Figure 1A. The result is shown in Figure 4A (a view from above). The add-a-point technique was also used to project points corresponding to a random sample of triangles. Figure 4B show views from the side to show some of the complexity of the surface.

The center of this space corresponds to an equilateral triangle and the three arms correspond to the three kinds of isosceles triangles. The arms extend out to infinity to correspond to an isosceles triangle with one side of zero length. For p>3 the space will require more dimensions and will be much more complicated and difficult to visualize. As in the previous section, there will be m arms extending out to infinity and "webs" connecting all pairs, triples, *etc.* of arms reflecting the possibility that any pair, triple, *etc.* of edges could tend towards zero simultaneously. As before, the central point in the space corresponds to a shape with equal inter-fandmark distances but for p>3 (2D data) or p>4 (3D data) such shapes are not

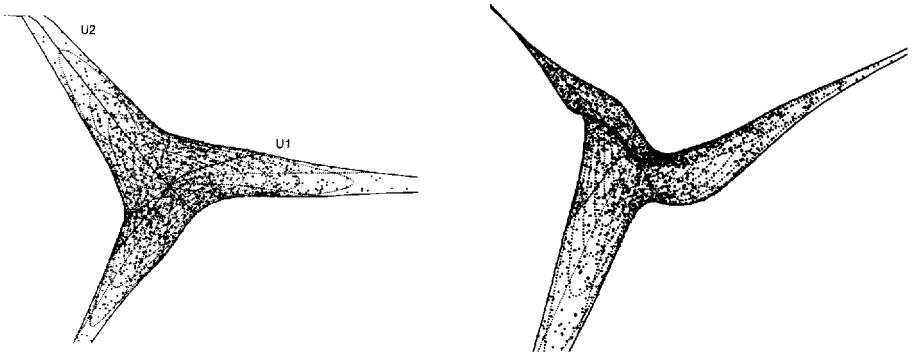

A *B*

Figure 4. Perspective views of the EDMA-I shape space for triangles. ***A.*** Top view. *B.* View somewhat from the side. The center corresponds to an equilateral triangle. The points correspond to a random sample of 2000 triangles.

physically realizable. There is again a gap in the center of this space that needs to be taken into account.

Lele and Cole (1995; 1996) proposed an alternative statistic, **Z,** which is the maximum absolute value **of** the arithmetic difference between the two size-scaled average form matrices being compared. They call this approach EDMA-11. They found that scaling by the length of a baseline resulted in higher power than scaling by centroid size. This method was proposed (Lele and Cole, 1996) as a method with higher power than EDMA-I and their postings on the morphmet listserver claimed it had much higher power than generalized T^2-tests using Bookstein shape coordinates. These results are in error due to a bug in their software (Rohlf 2000). The procedure described above was carried out to visualize the shape space implied by the Z-statistic (both centroid size and baseline size scaling were used). The results are shown in Figure 5 (A and B give perspective views of the space

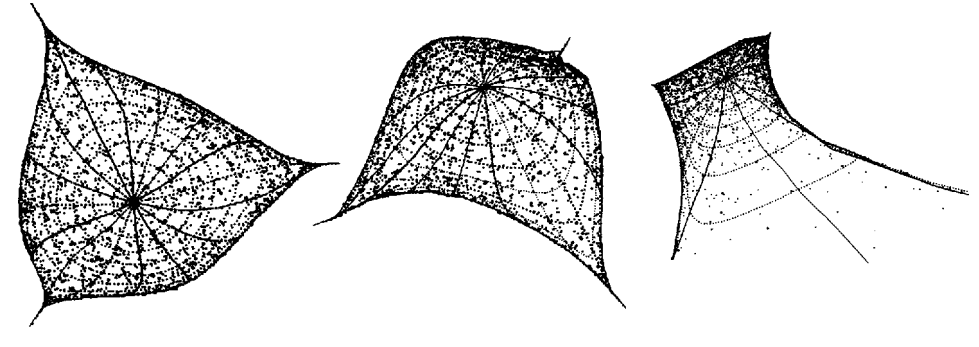

A *B* C

Figure 5. Perspectives view of the EDMA-II shape space for triangles using centroid size scaling. ***A.*** Top view. *B.* View somewhat from the side. C. Top view using the length of the **AB** baseline for sire scaling. The center corresponds to an equilateral triangle. The points correspond to a random sample of 2000 triangles.

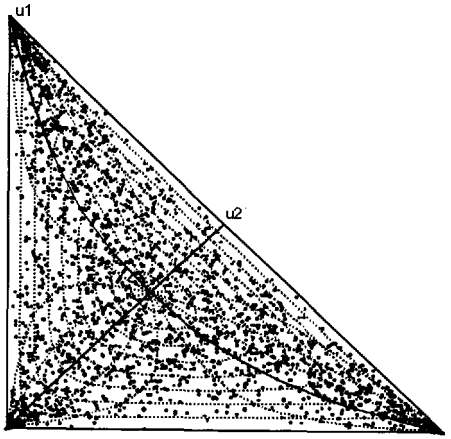

Figure 6. Shape space for triangles based on two of the interior angles (Rao and Suryawanshi, 1998). The point at the center corresponds to an equilateral triangle. The grid is as in previous **figures.** The points correspond to a random sample of 2000 triangles.

based on centroid size scaling and C gives a similar plot when the length of the **AB** baseline is used for size scaling. **As** before, the center corresponds to an equilateral triangle and the three arms correspond to the three kinds of isosceles triangles. However, the arms do not extend out to infinity unless baseline scaling is used. For $p>3$ (2D) or $p>4$ (3D) there will be a gap at the center of this shape space.

Recently, Richtsmeier et al. (1998) proposed another shape statistic, the square root of the sum of squared differences between the logs of size-scaled distances. This leads *to the same* shape space as the Rao and Suryawanshi (1996) method described above.

Differences in angles

Rao and Suryawanshi (1998) proposed that a natural method of comparing shapes is to compare angles from a triangulation of landmarks. Because the three angles in a triangle sum to a constant (π radians), only two arbitrarily selected angles are used from each triangle to be used as shape variables. Samples of shape are then compared by using standard multivariate methods on these shape variables. While several transformations are suggested that should reduce departures from normality, their examples are based on the raw angles. Figure 6 illustrates their shape space for triangles. Note that the distribution of random triangles is not uniform — the density is much higher in the three corners (corresponding to isosceles triangles) than along the sides (corresponding to oblique triangles).

STATISTICAL MODELS

The random samples of all possible shapes used in the previous section are useful to study the metric geometry of a shape space but they do not correspond to reasonable models for the type of variation one expects to find in practical applications. Goodall's (1991) perturbation model is a simple alternative. In this model the $p \times k$ matrix of coordinates for the ith specimen are given by

$$\mathbf{X}_i = \alpha_i(\mu + \mathbf{E}_i)\Omega_i + \mathbf{1}\omega_i^t \qquad (2)$$

where α_i is a scale factor (size), μ is the mean shape, $\mathbf{E}_i$ is a matrix of zero-mean Gaussian displacements, Ω_i is a $k\times k$ rotation matrix (reflections excluded), $\mathbf{1}$ is a vector of all ones, and ω_i is a vector corresponding to translation of the specimen. Parameters α_i, Ω_i, and ω_i are nuisance parameters whose effects are to be ignored when studying shape variation. Matrix $\mathbf{X}_i$ when strung out as a vector has a covariance matrix $\Sigma = \Sigma_p \otimes \Sigma_k$, where Σ_p is the covariance matrix for the landmark points (the rows of $\mathbf{E}_i$) and Σ_k is the covariance matrix for the dimensions (the columns of $\mathbf{E}_i$). In this study only the simplest case was investigated — independent homogeneous variation around each mean landmark position **such** as what one might expect from digitizing error ($\Sigma_p = \sigma^2\,\mathbf{I}$ and $\Sigma_k = \mathbf{I}$). This model was

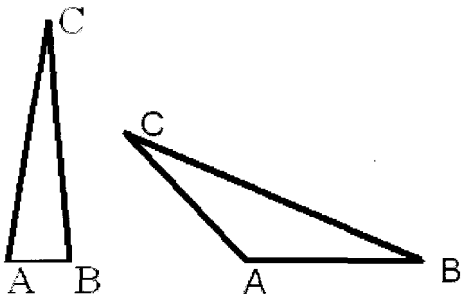

A B

Figure 7. Triangles used as the mean shapes in the sampling experiments and the figures that follow. A. An isosceles triangle. *B*. **An** oblique triangle. Both triangles are at a Procrustes distance of $\rho=\pi/6$ from an equilateral triangle.

investigated not because it is always reasonable biologically but because such a null model enables us to investigate distortion introduced by various methods of shape analysis. If a method seems to reveal interesting covariation patterns under this model then they must be due to an artifact of the method.

For Kendall shape space this model generates circular scatter around the position corresponding to the mean shape. Kendall tangent space also yields circular scatter as long as the point of tangency is close to the mean (as it should be in most practical applications). For example, the isosceles triangle in Figure **7A** (using $\sigma = 0.05$) produces the scatter shown in Figure 8A (the skewed triangle would show the same scatter if the point corresponding to its mean were used as the point of tangency. If the point of tangency were taken far from the sample mean, the scatter would become elliptical with its principal axis orthogonal to the direction towards the origin.

The stereographic projection of a distribution with circular density contours in Kendall shape space always yields a distribution with circular density contours because a stereographic projection is a conformal mapping (a transformation that preserves angles). However, unless the point of tangency is at the mean, the density contours will not be concentric and the distribution will be skewed away from the origin. Bookstein shape coor-

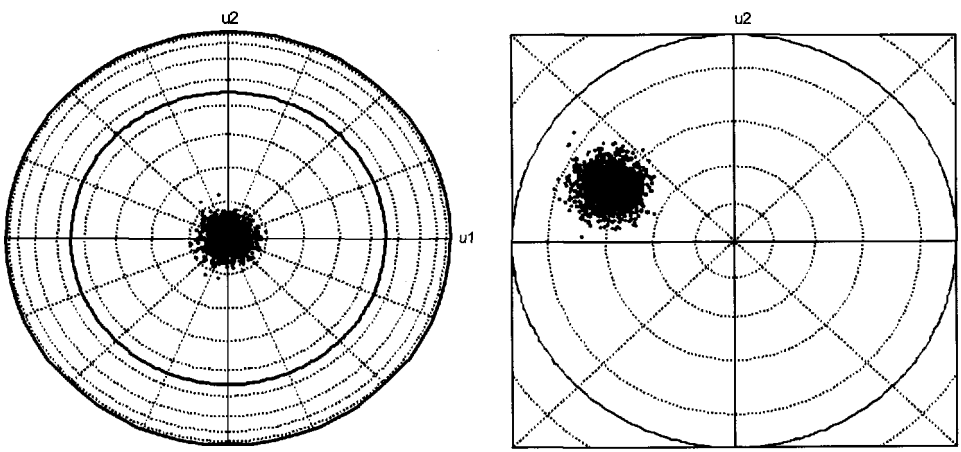

A B

Figure 8. Tangent space with a distribution of 2000 random triangles superimposed. The isosceles triangle in Figure **7A** was used as the mean shape. *A*. Kendall tangent space with the mean shape used as the reference. *B*. Stereographic projection corresponding to Bookstein rhape coordinates (edge BC used as the baseline).

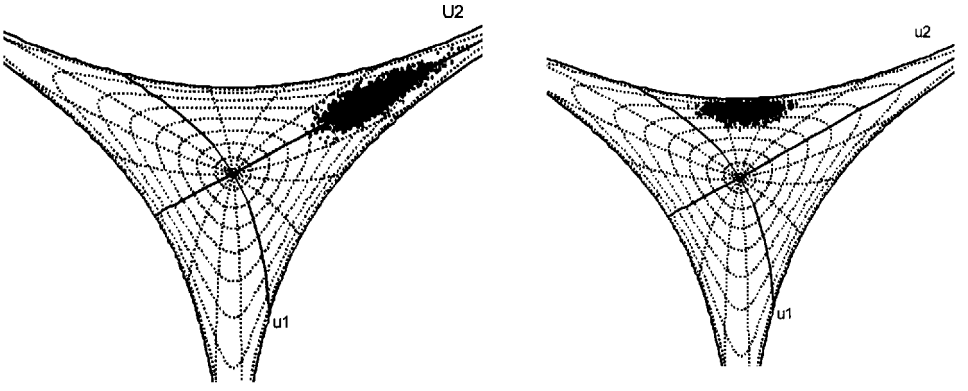

A ***B***

Figure 9. Shape space based on shape variables defined by Rao and Suryawanshi (1996) with the distribution of 2000 triangles superimposed. ***A.*** Distribution using the isosceles triangle in Figure 7A as the mean. *B.* Distribution using the oblique triangle in Figure 7B as the mean.

dinates are a special case. They correspond to using as a reference the collinear triangle with the free point at the origin and using a baseline defined by the other two landmarks, The skewness is very noticeable in Figure XB because the point of tangency is not very close to the mean shape. The variance of the scatter increases greatly for mean shapes further from the point of tangency (the standard deviation increases with the square of the distance). If a stereographic projection using the mean shape as the reference were used then the resultant distribution would resemble Figure 2B but with a smaller variance.

The results are very different for the other shape spaces examined. Figure 9 shows the distribution of points for the shape variables defined by Rao and Suryawanshi (1996). Figure 10 shows the projections of the same points onto the shape space implied by the EDMA-I statistic. Similar strong patterns

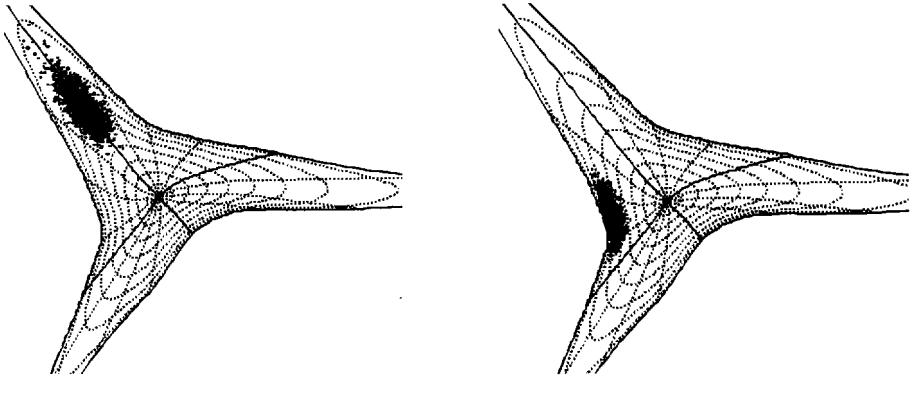

A ***B***

Figure 10. **A** perspective view of EDMA-I shape space with distributions of 2000 random triangles superimposed ***A.*** Distribution using the isosceles triangle in Figure 7A as the mean. *B.* Distrihution using the skewed triangle in Figure 7B as the mean.

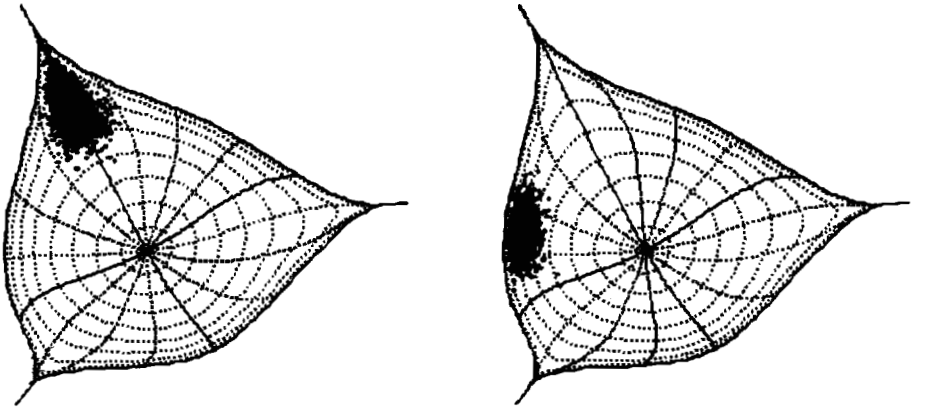

A *B*

Figure 11. A perspective view of EDMA-II shape space using centroid size scaling with distributions of 2000 random triangles superimposed. *A*. Distribution using the isosceles triangle in Figure 7A as the mean. *B*. Distribution using the oblique triangle in Figure 7B as the mean.

are shown in Figure 11 for the EDMA-II statistic using centroid size scaling and in Figure 12 for baseline size scaling. Figure 13 shows the same samples of points using two angles as shape variables as suggested by Rao and Suryawanshi (1998). The orientation of the scatter would be quite different if a different pair of angles were selected. In all of these examples, the size and orientation of the sample points are strongly influenced by the location of the mean in shape space.

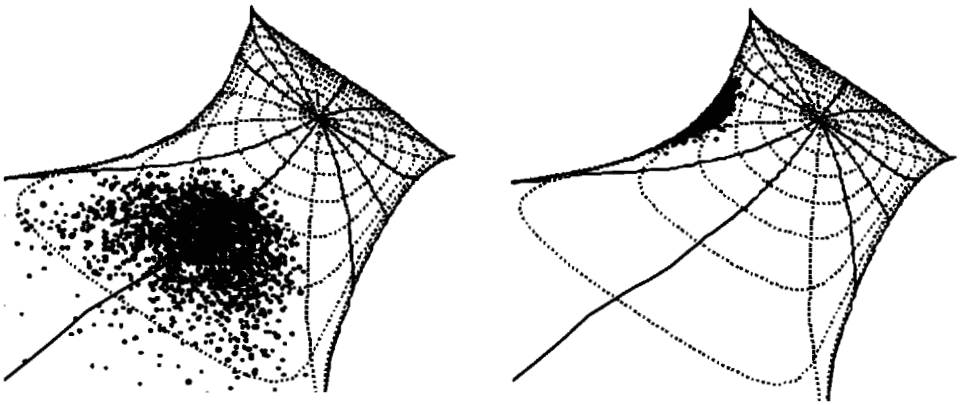

A **B**

Figure 12. **A** perspective view of EDMA-II shape space using baseline scaling with distributions of 2000 random triangles superimposed. **A.** Distribution using the isosceles triangle in Figure 7A as the mean and the basal edge as size. *B*. Distribution using the oblique triangle in Figure 7B as the mean.

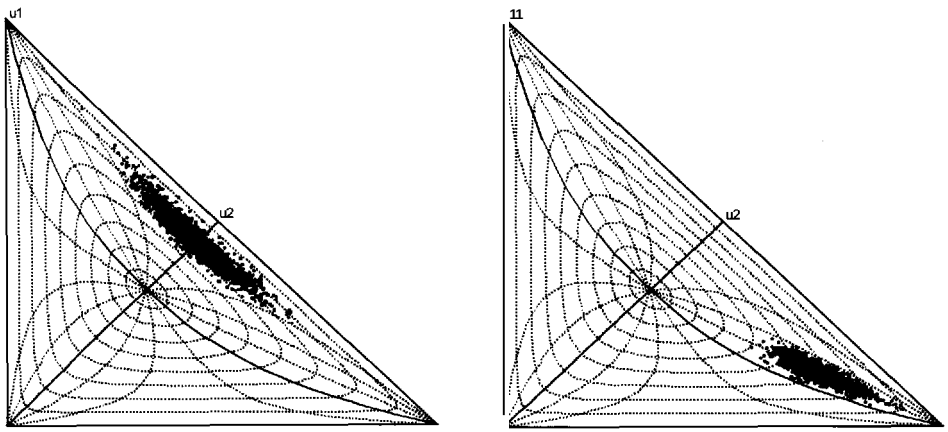

Figure 13. Shape space based on angles as defined by Rao and Suryawanshi (1998) with a sample of 2000 triangles superimposed **A.** Distribution using the isosceles triangle in Figure 7A as the mean. *B.* Distribution using the oblique triangle in Figure 7B as the mean. The angle at landmark **A** is plotted along the abscissa and the angle at B is plotted along the ordinate (other choices would give different results).

DISCUSSION

Rao and Suryawanshi (1996, 1998) suggested the use of traditional methods of multivariate analysis (D^2, MANOVA, CVA, *etc.)* to test for shape differences using their shape variables (log size-scaled interlandmark distances or angles from a triangulation). Unless the mean shapes are very similar (ideally with inter-landmark distances nearly equal so that the distributions of points are near the center of their shape space), this is unlikely to work well because the pattern of covariance is strongly influenced by mean shape. When the mean shapes are different, covariance matrices will be heterogeneous and that makes standard statistical tests inappropriate. Although it may not be detectable in practical applications where sample sizes are small, distributions can be far from multivariate normal depending upon the location of the mean in shape space. Figure 9B shows an example of a distribution whose density contours would be concave on the side away from the center of the space. The use of bootstrap and permutation test methods (such as used by Lele and Richtsmeier, 1991, and Lele and Cole, 1996) seems to be a more reasonable approach for testing statistics with such properties.

Another problem caused by the non-linearity of the shape space is that a simple average of a sample of shape variables can be a poor estimate of the true shape. If the mean shape for the distribution in Figure 9B were further from the center of the space then the sample average would be located outside of much of the region of high density. **As** Rao and Suryawanshi (1996) point out, the average can even be impossible — outside of the space of physically realizable shapes. For example, the average of isosceles triangles in two different arms of the Rao and Suryawanshi (1996) shape space can yield a point outside of their shape space because the space is not convex. In such cases, they suggest an ad hoc procedure using metric scaling (*e.* g., principal coordinates analysis, Gower, 1966) to obtain **a** valid shape. Lele

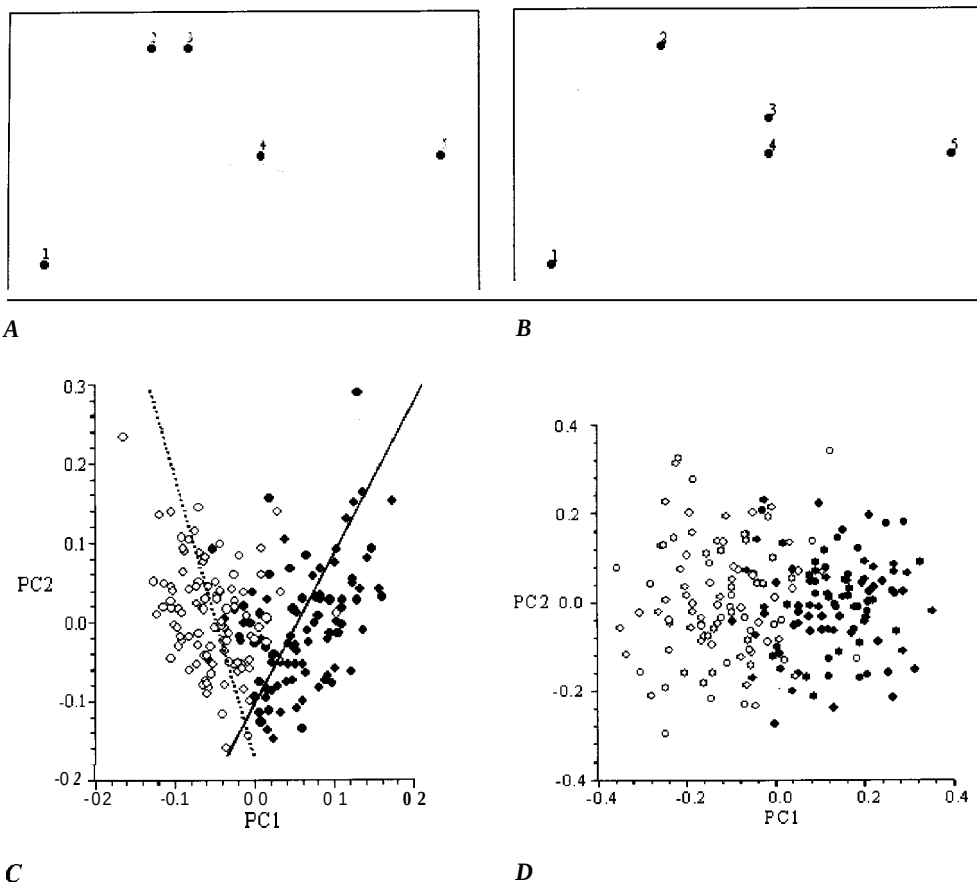

Figure 14. Sampling experiment to demonstrate effect of mean shape on covariation in the Rao and Suryawanshi (1996) shape space. *A.* Mean configuration of landmarks for population 1. *B.* Mean configuration for population 2 (landmark 3 moved). C. Projection onto the first two principal component axes of the Rao and Suryawanshi (1996) shape space with 100 observations from each population. The first principal component axis for each population are shown. *D.* Plot of the first two relative warp axes (PCA of Kendall's tangent space). Within-group principal component axes are not shown because the distributions are circular. Population 1 shown with filled circles (•) and population 2 shown with open circles (o).

(1993) makes a similar suggestion for the EDMA methods. This problem is caused by the fact that these methods do not properly take the non-linearity of shape space into account. These problems do not arise when working with Procrustes methods and Kendall shape space.

Morphometric studies using ordination analyses such as principal components or principal coordinates analysis also need to take the metric geometry of shape space into consideration. One cannot give a biological interpretation to the fact that one sample has a larger variance than another sample or that one sample has the same or different principal components than another without taking into account any constraints or distortions due to the shape space itself. A simple artificial example may be useful to show the importance of this point. Figure 14A and

B show the mean configurations of landmarks in 2 populations (they differ only in the location of landmark 3). A random sample of 100 observations from each population was simulated by adding homogeneous uncorrelated normally distributed error at each landmark. The Rao and Suryawanshi (1996) shape variables were computed and a principal components analysis performed using all 200 observations. Figure 14C shows the projections onto the first two principal component axes. The first within group principal components are also shown. The distributions are elongated due to the fact that the interlandmark distances are not equal (inter-landmark distances 2 – 3 or 3 – 4 are much smaller than the distances between other landmarks). The orientation of the scatter for the two populations are different because a different pair of landmarks has the shortest inter-landmark distance and thus are located in different arms of the shape space. Thus, as we have seen before, the covariance structure depends upon the mean shape. Tests for shape differences would be complicated by having to allow for heterogeneous covariance matrices. Rao and Suryawanshi (1996, 1998) ignore this problem and compute pooled within-groups covariance matrices. This is expected to cause a loss in power. If Figure 14C was the result of an actual biological application, a researcher would undoubtedly try to find a biological explanation for the elongated scatters and their differences in orientation. Any real differences in the covariation in the two samples would have to be fairly strong in order to be detectable. A comparable analysis of the points projected onto Kendall's tangent space (an analysis of relative warps) yields two more or less circular scatters (see Figure 14D). The first within group principal component axes are not shown because the scatters are circular and thus their directions poorly defined. This is the kind of result one would wish to obtain for populations that differ only in mean shape and all variation within groups is due to homogeneous uncorrelated error at each landmark.

In studies of growth or of evolutionary trajectories it is even more important take the metric geometry of shape space into account. Trajectories must remain within the space or they may yield nonsensical results (i.e., physically impossible configurations of points). Ad hoc adjustments such as principal coordinates analysis may yield feasible shapes but the shapes will then no longer necessarily lie along the estimated trajectory. Richtsmeier and Lele (1993) argue that the fact that their approach can yield impossible shapes is a desirable feature because they believe that discovering that an estimated form is impossible could be used to answer questions concerning constraints on physical systems. Actually, obtaining an impossible estimated shape only shows that the method of estimation is not sensible. It is unreasonable to expect trajectories in a nonlinear space to follow straight lines or other simple curves that do not take the geometry of shape space into account. When using Kendall's shape space one also needs to take its curvature into account. The simplest trajectories would be great circles. If shape variation is small enough (as it usually is), then the Kendall tangent space approximation will be satisfactory and one can test how well the trajectories can be approximated using standard regression methods. The tpsRegr software (Rohlf, 1998a) can be used to fit straight lines. Other software can be used to fit curves or piece-wise straight lines as required by biological considerations. The problem of geometrically impossible shapes will not arise so that one can concentrate ones attention on biological issues.

The study of various proposed alternatives to Kendall's shape space makes one appreciate the rigor and insight of Kendall's work. Alternative models will no doubt continue to be proposed. It would be helpful if such proposals included comparisons against existing methods.

ACKNOWLEDGEMENTS

The critical comments by Fred L. Bookstein on an early draft of this paper are gratefully acknowledged. The comments by Dean Adams through the many revisions of this manuscript were very helpful as were those of Leandro Monteiro and John Kent. Thanks also to Dennis Slice for comments and for sharing the results of his simulations of Kendall's shape space for triangles. This work was supported in part by a grant from the Ecological and Evolutionary Physiology (IBN-9728160) program of the National Science Foundation. This paper is contribution no. 1043 from the Graduate Studies in Ecology and Evolution, State University of New York at Stony Brook.

REFERENCES

Bookstein, F. L., 1991. Morphometric tools for landmark data: Geometry and Biology. Cambridge Univ. Press, New York.

Cole, T. M., III., 1996. Historical note: early anthropological contributions to "geometric morphometrics". Amer. J. Phys. Anthr., 101: 291-296.

Dryden, I. L., and Mardia. K. V., 1992. Size and shape analysis of landmark data. Biometrika, 79: 57-68.

Dryden, I. L., and Mardia, K. V., 1998. Statistical shape analysis. John Wiley and Sons, New York.

Goodall, C. K., 1991. Procrustes methods in the statistical analysis of shape (with discussion and rejoinder). J. Koy. Stat. Soc., Series B, 53: 285-339.

Gower, J. C., 1966. Some distance properties of latent root and vector methods used in multi-variate analysis. Biometrika, 53:325-338.

Gower, J. C., 1968. Adding a point to vector diagrams in multivariate analysis. Biometnka, 55: 582-585.

Gower, J. C., 1975. Generalized Procrustes analysis. Psychometrika, 40: 33-51.

Jackson, J. E., 1991. A user's guide to principal components. John Wiley and Sons, New York.

Kendall, D. G., 1981. The statistics of shape. In: Barnett, V. (ed.), Interpreting multivariate data. Wiley, New York: 75-80

Kendall, D. G., 1984. Shape-manifolds, Procrustean metrics and complex projective spaces. Bull. London Math. Soc., 16: 81-121.

Kendall, D. G., 1985. Exact distributions for shapes of random triangles in convex sets. Adv. Appl. Prob., 17: 308-329.

Kent, J. T., 1994. The complex Bingham distribution and shape analysis. J. Roy. Statist. Soc., B, 56: 285-299.

Lele, S., 1993. Euclidean distance matrix analysis: estimation of mean form and form difference. Math. Geol., 25: 573-602.

Lele, S., and Cole, T. M., III., 1995. Euclidean distance matrix analysis: a statistical review, SISA, Vol. 3, Univ. of Leeds, UK: 49-53

Lele, S., and Cole, T. M. III., 1996. A new test for shape differences when variance-covariance matrices are unequal. J. Hum. Evol., 31:193-212.

Lele, S., and Richtsmeier, J. T., 1991. Euclidean distance matrix analysis: a coordinate free approach for comparing biological shapes using landmark data. Amer. J. Phys. Anthr., 86: 415-427.

Marcus, L. F., Corti, M., Loy, A., Naylor, G. J. P. and Slice, D. E., 1996. Advances in morphometrics. Plenum, New York.

Rao, C. R., and Suryawanshi, S., 1996. Statistical analysis of shape of objects based on landmark data. Proc. Nat. Acad. Sc., 93:12132-12136.

Kao, C. R., and Suryawanshi S., 1998. Statistical analysis of shape through triangulation of landmarks: a study of sexual dimorphism in hominids. Proc. Nat. Acad. Sci., 95: 4121-4125.

Reyment, R. A., Blackith, R. E. and Campbell, N. A., 1984. Multivariate Morpho-

metrics. 2 ed. Academic Press, London.

Richtsmeier, J. T., Cole, III, T. M., Valeri, C. J. and Lele, S., 1998. Preoperative morphology and development in sagittal synostosis. J. Cran. Gen. Devel. Biol., 18: 64-78.

Richtsmeier, J. T., and Lele, S., 1993. A coordinate free approach to the analysis **of** growth patterns: models and theoretical considerations. Biolo. Rev, 68: 381-411.

Rohlf, F. J., 1996. Morphometric spaces, shape components and the effects of linear transformations. In: Marcus, L. F.. Corti, M., Loy, A., Naylor, G. J. P. and Slice, D. E. (eds.), Advances in morphometrics, Vol. 284, Plenum, New York: 117-129.

Rohlf, F. J., 1998. tpsREGR: Thin-Plate Spline Regression. Department **of** Ecology and Evolution, State University of New York at Stony Brook, Stony Brook, New York.

Rohlf, F. J., 1999a. Shape statistics: Procrustes superimpositions and tangent spaces. J. Class., in press: 000-000.

Rohlf, F. J., 1999b. tpsTri. Department of Ecology and Evolution, State University of New York at Stony Brook, Stony Brook, NY.

Rohlf, F. J., 2000. Statistical power comparisons among alternative morphometric methods. Amer. J. Phys. Anthr., 16: 197-223.

Rohlf, F. J.. and Marcus, L. F., 1993. A revolution in morphometrics. Trends Ecol. Evol., 8: 129-132.

Small, C. G., 1996. The statistical theory of shape. Springer, New York.